IEEE Transactions on Nuclear Science, Vol. NS-28, No. 3, June 1981

DESIGN AND OPERATION OF THE 100 MeV ALADDIN MICROTRON INJECTOR*

M.A. Green, E.M. Rowe, W.S. Trzeciak, and W.R. Winter
UW Synchrotron Radiation Center
3725 Schneider Drive
Stoughton, WI 53589

Summary

At present the Synchrotron Radiation Center (SRC) is nearing completion of its Aladdin project to provide a 1 GeV electron storage ring for the production of synchrotron radiation; the injector for this machine is a 100 MeV racetrack microtron (RTM). The choice of an RTM for this purpose if multifold: monoenergiticity of the output beam; basic simplicity of design; ease of operation; and reasonable cost. It is also for these same reasons that our facility has previously built two conventional (circular orbit) microtrons, used in the same application, at energies of 10 and 45 MeV.

Introduction

Although RTM's can have many different configurations, for the present application the simplest design is sufficient. Referring to Figure 1, this basically consists of a linac accelerating structure and two dc 180 degree bending magnets plus provision for injection, extraction, and vacuum and monitoring systems (not shown). Other RTM geometries differ mainly in the number and placement of bending magnets and the inclusion of magnetic quadrupole lenses. In contrast, the conventional microtron uses a single 360 degree magnet and a single rf cavity included within the magnetic field.

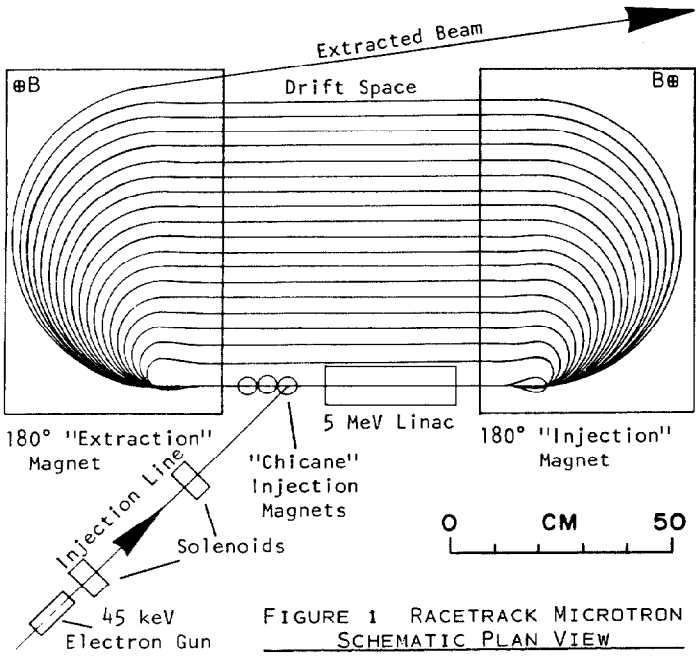

FIGURE 1 RACETRACK MICROTRON SCHEMATIC PLAN VIEW

As the present RTM design essentially represents the conventional microtron with the inclusion of a drift space, there are numerous operational similarities between them. Details of conventional microtron operation can be found in Ref. 1 and extended to the present case.

In particular, nearly the same description of phase stability applies in both cases. Lowest mode operation entails the lengthening of each successive orbit by one rf wavelength ($\lambda=c/f$). This condition is satisfied if the dc magnetic field (B) is related to the energy gain per turn (ΔE) by:

$$(\Omega\equiv)\ B/B_o = \Delta E/E_o \qquad (1)$$

where: $E_o = m_o c^2$, the electron rest mass energy

$B_o = (2\pi f)m_o/e$, the electron cyclotron field

$\simeq$ 1 kG at 3 GHz.

Relative to the peak of the accelerating wave the phase (ϕ) at which an electron passes through the linac is here described by

$$\Delta E = \Delta E_{max}\cdot\cos\phi\ . \qquad (2)$$

Maximum phase stability occurs on the falling portion of the wave where the stable phase angle (ϕ_s), and the maximum excursions of the phase ($\delta\phi$) and energy (δE) are approximately given by

$$\begin{aligned}\phi s &\simeq 20^\circ\\ \delta\gamma &\simeq \pm 15^\circ\\ \delta E &\simeq \pm .08\cdot\Delta E\ .\end{aligned} \qquad (3)$$

The relative advantage of the RTM design is seen by considering the importance of the principal operating parameter Ω (cf. Eq. 1). In a machine with N orbits, final energy (E_f) is approximately given by

$$E_f = N\Delta E = N\Omega E_o.$$

In the conventional microtron: 1) N is limited by consideration of a) possible phase resonance instability for $N \gtrsim 20$ to 30 orbits; and b) required magnetic field homogeneity $\propto 1/N^2$; and 2) Ω is limited by present injection methods to a value $\approx 2.0 \rightarrow 3.0$. Therefore, for the conventional microtron it is difficult to exceed

$$E_f \simeq (20)(2.0)(.511) \rightarrow (30)(3.0)(.511) \simeq 20 \rightarrow 45 \text{ MeV}.$$

Higher values of E_f realistically require higher Ω values. In RTM's where injection, acceleration, confinement, and hence Ω are not restricted, higher energies without necessarily increased size (final orbital radius) are possible.

Table I. Superficial Values for the Aladdin RTM

Symbol	f	Ω	B_o	B	ΔE	N	$E_f \pm \delta E$
Value	2800	10	1	10	5	20	101 ± .4
Units	MHz	-	kG	kG	MeV/Turn	-	MeV kinetic

Design Philosophy

Magnets

The magnetic structure satisfies many requirements: 180° bending of the beam, field termination in the "field free" drift space, low energy vertical focusing, high energy vertical focusing, colinear 180° injection bend, extraction angle, and simple means of correcting unwanted field perturbations. Despite these constraints, however, the magnet system is relatively simple. In the following discussion refer to the plan view of a magnet in Fig. 2, and the cross section of a magnet shown in Fig. 3. Figure 4 shows a graph of the magnetic field as keyed to Fig. 3.

Only one magnet is illustrated in detail as both magnets are identical in construction and magnetic fields but mirror images of each other. Except for the local field perturbation at the recesses, all field cross sections (cf. Fig. 4) are the same. In either magnet this translational symmetry implies normal exit for normal entry, a prerequisite of the closed orbit motion. Using identical magnets precludes any damaging

0018-9499/81/0600-2074$00.75©1981 IEEE

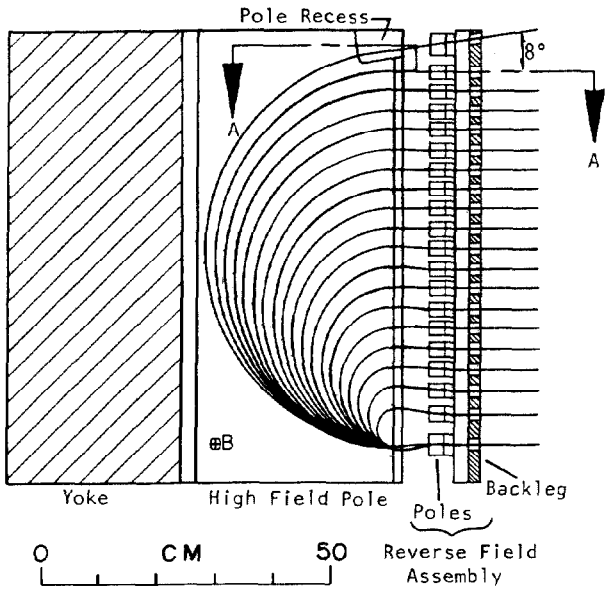

FIGURE 2 PLAN VIEW OF 180° (EXTRACTION) MAGNET
Section A-A is shown in Figure 3.

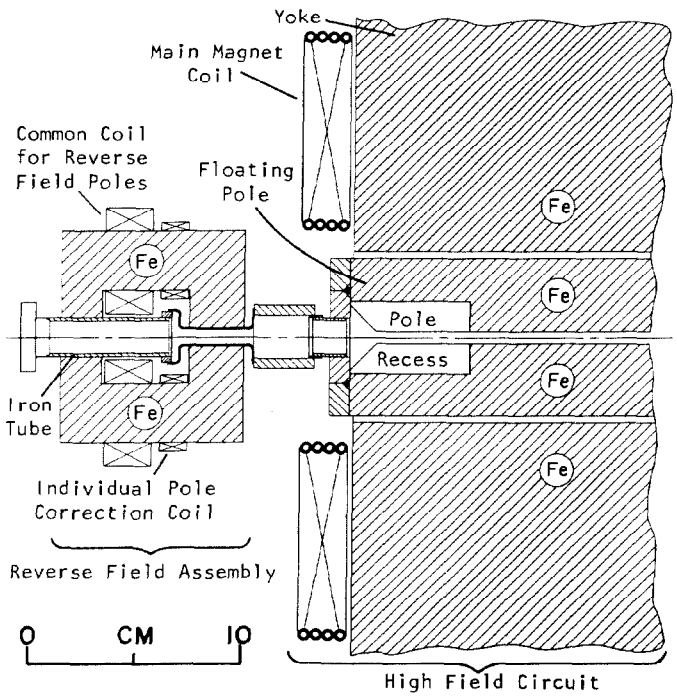

FIGURE 3 MAGNET CROSS SECTION A-A
- showing partial vacuum chamber assembly

field asymmetry; corrections in one magnet are duplicated in the other.

Note that "a magnet" here refers to the structures producing the main high field region and the reverse field region along the leading edge. As seen in Fig. 4 the main field is effectively truncated by this second structure preventing any undesirable effects on the phase motion. What's more, the reverse field causes angular entry into the main high field region such as to produce vertical edge focusing, at least at low energy before dissipating as the beam becomes stiffer on later orbits. The strength of this effect is determined mainly by $\int B \cdot dl$ through the reverse field region. The higher this deflection the greater the edge focus-

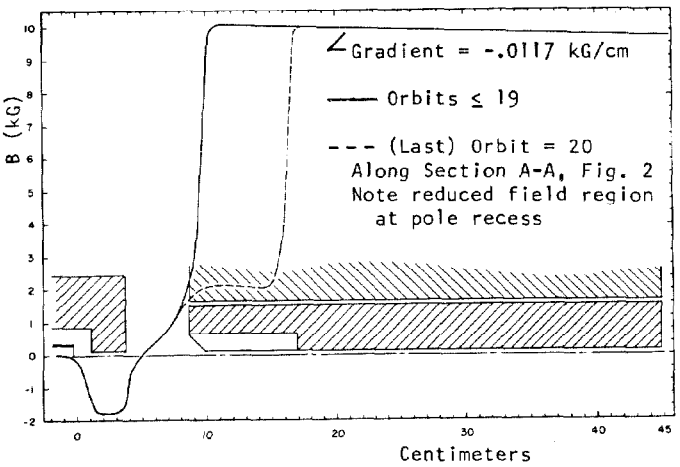

FIGURE 4 MEDIAN PLANE MAGNETIC FIELD PROFILES
- superimposed on magnet cross section of Figure 3

ing. The spacing of this reverse field region back from the leading edge of the main field is used to properly execute a colinear 180° bend of the injected beam in the first (injection) magnet (see Fig. 1). Thence the beam passes once again through the linac for a total energy of about 10 MeV kinetic before first encircling the linac. This scheme (as we first observed on the Lund machine[2]) has the principal advantage of easily avoiding what is otherwise passage of the beam too close to the linac axis at 5 MeV on the first circuit. It does, however, suffer the disadvantage of translating energy spread into radial position spread of the beam.

The high field region is generated between pairs of "floating" poles in each main yoke. The auxiliary air gaps act as a Purcell filter and as an easily accessible means to magnetically shim any imperfections in the fields. From the leading to trailing edges the spacing between poles increases slightly such as to produce the very slight (≈4%) field reducing gradient seen in Fig. 4. This gradient produces persistent betatron-like high energy vertical focusing of the beam. Note from Eqs. 1 and 2 that an indirect consequence of this gradient is a gradual increase of the stable phase angle by a few degrees which is virtually harmless to stable phase motion. (No particular significance exists in the chamfered leading edge seen in Fig. 3.)

Extraction is effected by the local magnet recess and field depression (see Fig. 4) at the position of the last orbit as it leaves the (extraction) magnet. This loss of rotation causes beam exit at an angle of about 8° from the normal. Correction of magnetic fields outside the recess was necessary and principally involved a magnetic shunt (not shown) inside the recess.

Steering corrections for the closed orbit are provided for by small coils on individual reverse field poles at each orbit (see Figs. 2 and 3). (The larger coils on the reverse field poles are for their common excitation.) Generally, field contours on all orbits are held to within about 0.1% of each other. The corrections coils can produce $\int B \cdot dl$ values of about ±.7 kG·cm (corresponding to an angular deflection of about ±4 mr @ 50 MeV).

Linac

The rf structure (see Fig. 5) is a 6 cell π mode linac representing 5 MeV end-to-end energy gain to a synchronous relativistic electron. The starting point for the design was the 5 cell structure used on Spear II. Cell design was scaled down for operation at 2800 ± .5 MHz, and the outer walls squared off to pro-

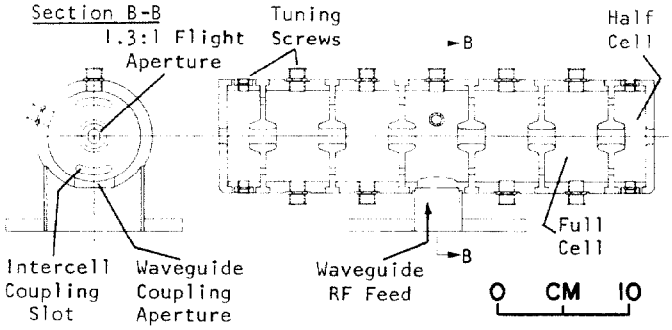

FIGURE 5 5 MEV LINAC

vide additional beam clearance on the first orbit to completely encircle the linac (cf. Fig. 1). The number of cells was chosen with the factors of reduced rf power, peak nose (electric) fields, size, and construction costs as considerations. Intercell coupling, $\gamma = 2\%$, is accomplished with azimuthal slots in the common walls. The external waveguide coupling parameter is presently $\beta_0 = 2.0$. These and other parameters are shown in the following table.

Table II: Linac Parameters

Symbol	Parameter	Value	Units
f	Frequency	2800	MHz
	No. of (Equivalent Full) Cells	6	
	Flight Aperture: Dia., Nominal	1	cm
	Aspect Ragio	1.3:1	
γ	Intercell Coupling Coefficient	2%	
β_0	Input Coupling Coefficient	2.0	
Q_L	Loaded Q	3040	
Q_o	Unloaded $Q_o = Q_L(1+\beta_0)$	9240	
ΔE	Energy Gain/Turn (ave.; taken at midpoint of acceleration)	5	MeV
	Peak Nose Electric Field	75	MV/m
	Pulse Length	2	μs
	Rep Rate, max	10	Hz
P	Power: During Pulse	1.8	MW
	Ave., max.	40	W

RF Source: 4.7 MW Varian 1137 Coaxial Magnetron and Surplus AN/FPS-6 Radar Set

A distinguishing feature of the linac is the flight apertures. Due to the translational symmetry of the magnets no radial focusing is produced there and such focusing must be provided elsewhere in the machine. In particular, the linac axis / orbital baseline is a region common to all orbits and can contain a radially focusing element. We have chosen to incorporate radial focusing in the linac by vertically elongated flight apertures having an aspect ratio of 1.3:1. Because this focusing accompanies the acceleration process, radial focusing occurs as the beam passes through the linac in either direction. This scheme does not preclude inclusion of an adjustable magnetic quadrupole on the baseline at a later time if needed.

Injection

Injection is straightforward and has its essential features patterned after the Lund design[2] (refer to Fig. 1 in the following). An external gun provides an unmodulated 45 keV beam of electrons during the rf pulse. Enroute to the linac the transport line passes through two focusing solenoids and steering magnets. A three magnet "chicane" with zero $\int B \cdot dl$ is used before the linac to inflect the very low energy beam through the linac while leaving higher energy ($\gtrsim$ 10 MeV) beam components relatively unaffected. Having passed through the linac once, acquiring a total kinetic energy of about 5 MeV, the beam is bent back on itself in the "injection" end magnet (see previous discussion above). Reentering the linac in the opposite direction effectively inserts the beam into the acceleration cycle.

Extraction

Removal of a beam from the microtron is also a simple matter. This is because diametral orbit spacing ($\simeq$ circumferential change per orbit $\div \pi = \lambda/\pi$) $\approx$ 3 cm here, and separate influence can be exerted uniquely on the last orbit. In particular (referring to the previous magnet discussion) the final orbit is bent 8° less than 180° through the "extraction" magnet and exits from the machine along this angle.

Establishing the Parameters

Computer simulation of the single particle motion was used to study this design and assign operating values to the many parameters.[3] These computations dictated the adjustment of all magnetic field parameters, relative positioning of the linac and each magnet for phasing control, and the elongation of the linac flight apertures. Criteria for these selections were phase stability near the desired ϕ_s value, good focusing control of the vertical motion, and positive radial focusing and stability of the beam.

Project Status

Because of scheduling delays the RTM injector is not yet operational, thus precluding a discussion of operation and future plans. At present, with the exception of the vacuum system, all major subsystems are complete and ready for assembly. Magnet field surveys and corrections are mostly completed. The linac has been tested at low excitation but not as yet at full gradient. Realistically, initial machine testing is now about one month away.

References

1. S.P. Kapitza and V.N. Melekhin, *The Microtron*, Harwood Academic Publishers, LTD.; London (1978).

2. Private communication. See also: R. Alvinsson and M. Eriksson, *A Design Study of a 100 MeV Race-Track Microtron/Pulse-Stretcher Accelerator System*, TRITA-EPP-76-07/LUSY-7601, Electron and Plasma Physics, Royal Inst. of Tech. Stockholm (Apr. 1976).

3. M.A. Green, *Orbit Studies for the 100 MeV Aladdin Racetrack Microtron Injector*, these proceedings.

#Work performed under NSF contract DMR-7708657.